

Unraveling Contagion Origins: Optimal Estimation through Maximum-Likelihood and Starlike Tree Approximation in Markovian Spreading Models

Pei-Duo YU, Chee Wei Tan*, Liang Zheng[†] and Chao Zhao[‡]

Chung Yuan Christian University, Nanyang Technological University*, Independent Researcher[†], City University of Hong Kong[‡]

peiduoyu@cycu.edu.tw, cheewei.tan@ntu.edu.sg*

Abstract—Identifying the source of epidemic-like spread in networks is crucial for tasks like removing internet viruses or finding the rumor source in online social networks. The challenge lies in tracing the source from a snapshot observation of infected nodes. How do we accurately pinpoint the source? Utilizing snapshot data, we apply a probabilistic approach, focusing on the graph boundary and the observed time, to detect sources via an effective maximum likelihood algorithm. A novel starlike tree approximation extends applicability to general graphs, demonstrating versatility. We highlight the utility of the Gamma function for analyzing the asymptotic behavior of the likelihood ratio between nodes. Comprehensive evaluations confirm algorithmic effectiveness in diverse network scenarios, advancing rumor source detection in large-scale network analysis and information dissemination strategies.

I. INTRODUCTION

Epidemic-like spreading represents a crucial topic in network science, extensively explored in the existing literature [1]–[3]. Specifically, the proliferation of malicious information in networks has emerged as a significant cybersecurity challenge [4]. Detecting the sources of malicious information has numerous applications, such as eradicating computer viruses or identifying the origins of rumors spreading on the Internet or online social networks. The COVID-19 pandemic marked a unique global crisis, intertwining the epidemics of the virus with an overwhelming surge of misinformation. It became the first pandemic in history that triggered an *epidemic of online misinformation*, which significantly undermined the efficacy of online social networks and disrupted public health risk communications [5]–[7]. In response, the World Health Organization (WHO) swiftly declared war against the COVID-19 Infodemic, referring to the viral spreading of pandemic-related misinformation or disinformation on social media [6].

The problem of identifying the origin of contagion was initially explored in the seminal work [8], [9]. The task at hand focuses on identifying the origin of a spreading event, given a single snapshot depicting the network of connections among individuals labeled as “infected,” based on the Susceptible-Infectious (SI) model described in [10] for contagion propagation. For simplicity, we will refer to nodes that have acquired the malicious information as *infected nodes* and those that have not as *susceptible nodes* or, alternatively, as *uninfected nodes*. This problem is framed as a graph-constrained

maximum likelihood estimation, intensified by the interaction between spreading dynamics and network topology, crucial for developing scalable, efficient algorithms, as highlighted in [7]. The concept of rumor centrality was first introduced in [8], [9] as a novel method for addressing the challenge of maximum likelihood estimation in the context of rumor spread analysis. This approach involves assigning a numerical value to each node within the network that has been exposed to the rumor, with the aim of identifying the node that possesses the highest value, designated as the *rumor center*. Specifically, the rumor center is the exact optimal solution for the maximum likelihood estimation problem for graphs embedded in infinite regular trees. The rumor center can be efficiently computed using message-passing algorithms, as described in [11]. Moreover, the effectiveness of this strategy can be evaluated asymptotically, particularly as the number of nodes affected by the rumor escalates significantly [8], [12].

The maximum likelihood estimation for general network topology remains unsolved, with only a few special cases having optimal solutions. These cases involve infinite underlying graphs with specific structures, such as degree-regular tree graphs [8] or starlike graphs [13], or special scenarios with finite underlying graphs [7], [14], or graphs containing cycles [7], [15]. However, some heuristics based on network centrality, such as those in [8], [9], [16], [17], have demonstrated good performance. Since the initial work by [8], [9], the problem formulations have undergone several modifications. For instance, generalizations to random trees were explored in [12], extensions with suspect sets were introduced in [18], and the problem was extended to multiple source detection in [19]. Furthermore, an extension for detection with multiple snapshot observations was studied in [20]. A comprehensive survey on this topic can be found in [7].

We consider a probabilistic approach to rumor source detection using a continuous-time SI model that shares similarities with the discrete-time SI model in [8], [9]. Both models share the feature that the time gap between the occurrence of a new infection and the immediate preceding one follows an exponential distribution with a constant mean. Other work employing similar models include [21], [22]. The fundamental concept of this paper is to define the *rumor boundary* of the observed rumor graph, facilitating a probabilistic method for

estimating the source. Specifically, source estimation can be effectively determined by a message-passing algorithm on tree networks. This introduces a unique method of characterization distinct from the centrality-based approaches introduced in prior works [8], [9], [16], [17]. The initial research presented in this paper was previously published in [23].

We summarized the main contributions of this paper as follows:

- We present a detailed probabilistic examination focusing on the boundary of the rumor graph. By analyzing the properties of graph connectivity and the effects of observation timing, we provide novel insights into the dynamics of rumor propagation in networked structures.
- We formulate the source detection problem as a maximum likelihood estimation by leveraging observed graph data and precise observation timings. We show that when the underlying network is a degree regular tree, the ratio of the likelihood of being the source between two nodes is independent of the observed time T . We propose a highly effective distributed message-passing algorithm tailored for tree networks, establishing its global optimality for starlike graphs.
- To address the challenge of maximum likelihood estimation for source detection in general graphs, we propose a novel starlike tree approximation for general graphs and then demonstrate the algorithm's performance in graphs with cycles. This extends its utility beyond tree networks, showcasing its versatility and robustness.
- Our formulation provides valuable insights into network resilience under complex system behavior at vast scales. In particular, we show that the asymptotics of gamma functions offer a potent tool for analyzing graph-theoretic features in large networks. Leveraging their properties enables the approximation of essential combinatorial quantities, facilitating the characterization of source estimation and detection.
- Our comprehensive performance assessment illustrates that the proposed algorithm achieves robust numerical results across different random graphs, including those with cycles and intricate boundaries.

Collectively, these contributions mark a significant advancement in the field of rumor source detection, offering valuable insights and methodologies that transcend traditional boundaries. This research paves the way for enhanced network analysis and information dissemination strategies.

The organization of this paper is as follows: Section II details the SI spreading model utilized in this study, incorporating an observed time variable T , and introduces the ML estimator for identifying the source. In Section III, we show that the likelihood ratio between two nodes in this temporal SI spreading model is independent of the observed time when the underlying network is a regular tree. Next, we analyze the likelihood of a specific node within the context of the rumor boundary and proceed to derive the ML estimator for tree graphs. In Section IV, we propose a starlike tree approximation for the source estimator in general graphs and analyze the likelihood ratio asymptotically. Section V assesses the

effectiveness of our probabilistic method for source estimation across various network structures. We further discuss other possible spreading distributions in Section VI. The paper is summarized in Section VII.

II. SYSTEM MODEL

In this section, we outline the rumor-spreading model and introduce a maximum likelihood (ML) estimator for identifying the source, focusing specifically on the impact of time on infected nodes, diverging from the approach used in [8], [9].

A. Rumor Spreading Model

In our study, the network is represented by an undirected graph $G = (V, E)$, with V being the node set and E comprising edges of the form (v_i, v_j) , for $v_i, v_j \in V$. The degree d_i of node v_i refers to the count of adjacent neighbors of v_i , and $d_G(v_i, v_j)$ denotes the graph distance (number of hops) between v_i and v_j in G . We assume a prior uniform probability for one out of all the nodes, denoted as the rumor source $v^* \in V$, to initiate the spreading at time $T = 0$.

The dynamics of rumor dissemination are represented through the susceptible-infected (SI) model, a simplification of the SIR model for disease transmission [10], which has two node types: susceptible, which can be infected, and infected, which spreads rumors to its neighbors. The infection spreads in a chain reaction, with each infected node permanently retaining and potentially transmitting the rumor to their susceptible neighbors. The time τ_{ij} takes for a node v_i to infect v_j is exponentially distributed. For simplicity, We assume each infection event is independent and with a standard rate λ .

B. Rumor Source Estimator

Assuming a rumor starts from a node v^* in a given network G at initial time $t = 0$ and propagates through it. By the time $t = T$, we observe G and identify N nodes as infected, forming a connected subgraph of G . We call G the underlying graph and G_N the rumor graph. Our objective is to propose a source estimator \hat{v} for deducing the origin of the rumor by considering the network structure and the observed time T . Utilizing Bayes' theorem, the ML estimator for v^* identifies the node that maximizes the probability of correct detection, as determined by

$$\hat{v} \in \arg \max_{v \in G_N} P(G_N | v, T), \quad (1)$$

where $P(G_N | v, T)$ represents the likelihood of observing the rumor graph G_N at time T , given v as the presumed source of the rumor. It should be noted that in the event of ties within the solution of the maximum likelihood estimation, they are resolved uniformly at random, indicating that the solution might not be singular.

III. RUMOR SOURCE DETECTOR FOR TREE GRAPHS

This section evaluates $P(G_N | v, T)$ in tree graphs. We need to compute a multiple integral with more than $N - 1$ variables when computing $P(G_N | v, T)$ for an N -nodes tree. We take Fig. 1 for example; the value of $P(G_4 | v_1, T)$ can be obtained

by calculating a multiple integral with nine variables since the graph has nine edges. To present the forthcoming theorem, we define the concept of a d -regular tree. A d -regular tree is defined to be a tree graph where each node has d neighboring nodes, hence a d -regular tree has infinite number of nodes. Here, we consider finite-size regular trees, where only leaf nodes may not have d neighbors. When the underlying network G is a regular tree and G_N does not contain any leaf node in G , the likelihood ratio between any two nodes is independent of the time T . In the following, we consider an example of G as a 3-regular tree and $G_4 \subset G$ is the observed rumor graph as shown in Fig. 1. We can observe that the first constant is the only difference between the likelihood of any two nodes in G_4 . Based on the observation, we present some theoretical results in a d -regular tree in the following, which coincides with the results in [8].

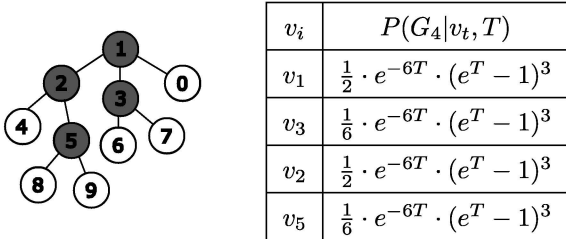


Fig. 1: An example rumor graph where the underlying graph is a 3-regular tree. The figure illustrates infected nodes as grey and susceptible nodes as white circles. It is important to note that the underlying graph could potentially extend infinitely, but this detail is omitted due to space constraints. The likelihood of each vertex that leads to the observed rumor graph G_4 is listed in the table on the right.

Lemma 1: Let G be a d -regular tree and $G_N \subset G$ be the observed rumor graph of G with no leaf node of G . For each $v \in G_N$, the likelihood $P(G_N|v, T)$ must have the following form

$$P(G_N|v, T) = k \cdot e^{-(N(d-2)+2)T} \cdot (e^{(d-2)T} - 1)^{N-1}, \quad (2)$$

for $N \geq 2$, and k is a number independent from T .

In Lemma 1, the term $(N(d-2)+2)$ in the power of the exponential means there are $(N(d-2)+2)$ uninfected neighbors of G_N in G and the term $N-1$ means there are $N-1$ infected edges, i.e., the edge connecting two infected nodes. For example, if G_N is on a 3-regular tree with $N=4$, then for all $v \in G_N$, we have $P(G_N|v_i, T) = k_i \cdot e^{-6T} (e^T - 1)^3$, where k is a scalar as shown in Fig. 1. To present the next result, we define $g_u^v \subset G_N$ to be the subtree rooted at u when we treat G_N as a rooted tree with root v , and we denote $|g_u^v|$ the number of nodes in the subtree g_u^v .

Theorem 1: Let G and G_N be defined as in Lemma 1. Then for any two adjacent nodes u and $v \in G_N$, we have

$$\frac{P(G_N|v, T)}{P(G_N|u, T)} = \frac{|g_v^u|}{|g_u^v|}.$$

The above Theorem 1 shows that when G_N is a subgraph of a regular tree, the likelihood ratio between two adjacent nodes in G_N is independent of the time T and only related to

the graph topology of G_N . Hence, we can find the maximum likelihood estimator for the source on G_N by only considering the structure of G_N , which leads to the same result in [8].

Next, we consider the case of general trees. Our goal is to approximate $P(G_N|v, T)$ by considering the nodes on the rumor graph boundary, and this also enables a message-passing algorithm. To analyze the *boundary* of the rumor graph, we first define the $d(v, G_N) = \min_{u \in G_N} d_G(u, v)$ to be the distance between a single vertex v and a subgraph $G_N \subset G$. For a given underlying G and a rumor graph G_N , we define the *rumor graph boundary* as follows.

Definition 1: Let $\mathcal{B}(G_N) = \{v \in G | d(v, G_N) = 1\}$, and we call $\mathcal{B}(G_N)$ the boundary of the rumor graph G_N . If a node $v \in \mathcal{B}(G_N)$ and the neighbor of v in G_N is not a leaf of G_N , then we call v a *pseudo-leaf* of G_N . Lastly, we define $\bar{G}_N = G_N \cup \{\text{all pseudo-leaves of } G_N\}$, and call \bar{G}_N the *rumor closure* of G_N .

Consider Fig. 1 as an example, the rumor graph boundary is $\mathcal{B}(G_4) = \{v_0, v_4, v_6, v_7, v_8, v_9\}$, where v_0, v_4 are pseudo-leaves. The boundary of the rumor graph offers valuable perspectives on the dynamics of rumor dissemination, characterized by probabilistic properties that significantly influence the detection of the rumor source.

A. Evaluation of Graph Boundary on Trees

Within a tree graph, if we treat the rumor source as the root of the tree, then the rumor spreading is limited to movement from parent nodes to their child nodes, simplifying the evaluation of $P(G_N|v, T)$. This means that rumor propagation within a tree structure is limited to a single path, unlike in general graphs where multiple paths are possible. As illustrated in Fig. 1, node v_5 is infected unless v_1 and v_2 were infected before. Furthermore, for being a leaf node, we must ensure that all child nodes of v_5 , i.e., v_8 and v_9 , are not infected by time T . Hence, we only need to consider the nodes on the boundary since they provide enough information about the rumor graph.

For simplicity in notation, we use v_i to indicate an infected node; conversely, \bar{v}_i denotes a node that is not infected. Hence, with the source node v_j (that is, the root of the rumor tree G_N) and a specific time T , the probability that node v_i act as a leaf in G_N and that all its susceptible children $v_l \in \mathcal{B}(G_N)$ can be calculated by

$$P \left(v_i \bigcap_{v_l \in \text{child}(v_i)} \bar{v}_l \mid v_j, T \right) = \int_0^T \frac{t^{K_{ij}-1} e^{-t}}{(K_{ij}-1)!} e^{-(T-t)(d_i-1)} dt, \quad (3)$$

where $K_{ij} = d(v_i, v_j)$. To grasp the concept presented in (3), it is crucial to acknowledge that the spreading time from v_j to v_i , represented by the sum

$$\tau_j + \dots + \tau_i$$

follows the Erlang distribution characterized by a shape parameter K_{ij} and a rate parameter λ , under the condition that each individual transmission time τ_j, \dots, τ_i is exponentially distributed with the same parameter λ . The probability density function of this Erlang distribution for $\lambda = 1$ is

$$\text{Erlang}(K_{ij}, \lambda = 1) = \frac{t^{K_{ij}-1} e^{-t}}{(K_{ij}-1)!},$$

i.e., the first term in the integration of (3). Furthermore, the term $e^{-(T-t)(d_i-1)}$ guarantees that all $d_i - 1$ children of v_i remain susceptible at time T . For example, we can set $K_{5,1} = 2$, $d_5 = 2$ in (3) to compute the probability of v_5 being the leaf of G_4 in Fig. 1. On the other hand, if v_i is a pseudo-leaf, then we assume it is equivalent to the case that $\text{parent}(v_i)$ is a degree-2 leaf. Additionally, we introduce a simple but useful formulation for computing the likelihood between two adjacent nodes. Let u, v denote two adjacent nodes in a connected graph G_N , and (u, v) be a bridge in graph G_N . Then G_N can be composed of two connected subgraphs plus the bridge (u, v) , i.e., $G_N = G_N^1 \cup \{(u, v)\} \cup G_N^2$ where $u \in G_N^1$ and $v \in G_N^2$. We have

$$P(G_N|u, T) = P(G_N^1|u, T) \cdot \int_0^T e^{-x} P(G_N^2|v, T-t) dt. \quad (4)$$

The above equation provides a tool for comparing the likelihood between two nodes or when the likelihood of one of the neighbors is provided on its subgraph.

The following lemma shows the properties of (3).

Lemma 2: Given source v_j and at time T , the probability of a node v_i being a leaf node in the rumor graph G_N , but not a leaf in G , has the properties in terms of observation time T , the node depth in the tree K_{ij} and the degree of the node d_i .

- Given K_{ij} and d_i , (3) first increases then decrease to 0 as T increases to infinity.
- Given K_{ij} and T , (3) decreases with d_i .

The probability function described in (3) suggests that the likelihood of the rumor reaching the leaf node is greater when there is sufficient time. Intuitively, extending T provides the rumor more opportunity to propagate across successive edges within a specified distance K_{ij} . Conversely, a higher degree restricts the leaf node by increasing the number of susceptible child nodes it must maintain. Hence, as T increases from 0, the value of (3) also increases from 0 until it reaches its maximum, i.e., the current time T is “adequate” for the given $K_{i,j}$ which is around $K_{i,j} - 1$ since we assume that $\lambda = 1$. Then, the value of (3) starts decreasing to 0 in the long run, which means the probability of spreading the rumor to a finite amount of nodes that use infinite time is almost equal to 0. Hence, there will be no leaf node after a very long rumor-spreading time, meaning all nodes will be infected by then. The second property in Lemma 2 can be understood similarly. We illustrate the two statements in Lemma 2 by plotting the graph of (3) in Fig. 2 with different tuples of K_{ij} , d_i , and T .

B. Maximum Likelihood Estimation for Trees

In a specific scenario of G_N where the source node v serves as the root of the tree, the probability $P(G_N|v, T)$ can be determined solely based on the probabilities of all leaf nodes being infected by time T , as explained in the upcoming lemma.

Lemma 3: For any two leaves nodes v_i and $v_j \in G_N$, if the lowest common ancestor of v_i and v_j is the root v , then $P(v_i \cap v_j|v, T) = P(v_i|v, T) \cdot P(v_j|v, T)$. Otherwise, if $d(v_i, v) = d(v_j, v)$ and $T \leq d(v_i, v) - 1$, then we have $P(v_i \cap v_j|v, T) \geq P(v_i|v, T) \cdot P(v_j|v, T)$.

The above lemma states that the infection of v_i and v_j are independent of one another when the lowest common ancestor of v_i and v_j is the root node. Note that when both v_i and v_j are pseudo-leaves of G_N , we can have the same conclusion as above. We introduce a class of graphs such that the likelihood of its centered node can be computed efficiently.

Definition 2: A connected simple graph G is a *starlike graph* if G satisfies [24]:

- G has a spanning tree \mathcal{T} such that \mathcal{T} is homeomorphic to a star graph with the center node denoted as v_c .
- For each node $v \in G$, $d_G(v, v_c) = d_T(v, v_c)$.

For example, the star graphs considered in [13] are starlike trees. If both G and G_N are starlike trees, and G contains the centered node v_c of G , then we can compute $P(v_c|G_N, T)$ by simply multiplying the probability (3) for all leaves. To simplify the notation, we denote the integrand in (3) as $\hat{f}_i(v_j, t)$ for brevity. Note that the variables K_{ij} and d_i are not shown in \hat{f} since the value of K_{ij} and d_i are fixed as G_N , v_i and v_j are given. By Lemma 3, we have

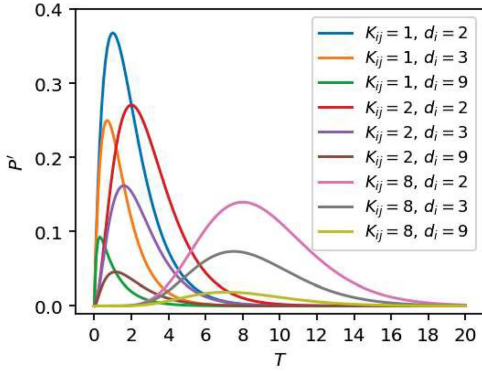
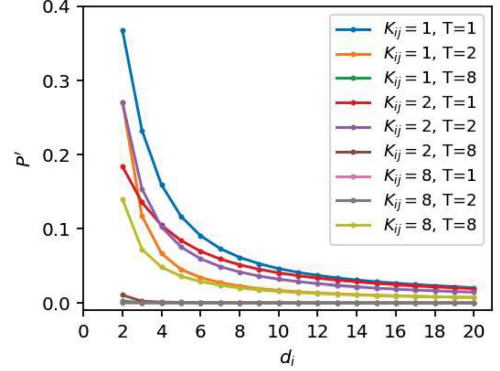
$$P(G_N|v_c, T) = \prod_{v_i \in \text{leaf}(G_N|v_c)} \left(\int_0^T \hat{f}_i(v_c, t) dt \right), \quad (5)$$

since for each pair of leaves, their lowest common ancestor must be v_c . In the following, we present a message-passing technique aimed at calculating a solution that might not be as optimal as the one in (1), but holds the potential to deliver the best possible global solution for certain graph topologies, such as line graphs or star-shaped graphs. This message-passing approach is motivated in part by maximizing the lower boundary mentioned in Lemma 3. Subsequently, we introduce a heuristic for starlike graphs, which approximates either a given tree graph or a general graph as a starlike configuration and then employ the message-passing technique.

C. Message-Passing Algorithm on Tree Graphs

To identify the source within a tree G_N , it is essential to compute the likelihood for all infected nodes. Under the assumption that nodes only obtain information from their immediate neighbors, we propose a message-passing algorithm that computes the likelihood of v being the source of G_N . The proposed algorithm includes two message-passing phases: top-down (from the root to leaves) and bottom-up (from leaves to the root). Each node v_i in the following algorithm has an attribute, i.e., the distance from the root k . Initially, the attributes k for all nodes are set to be 0 based on our assumption. The procedure is summarized in Algorithm 1.

During the initial top-down phase, which encompasses the first three steps in Algorithm 1, the root of the tree sends messages indicating the distance from itself to the (pseudo)leaves of \bar{G}_N , enabling the calculation of k for each node. Subsequently, in the bottom-up phase, each node collects the probabilities received from its children and passes this aggregated information to its parent. This process is repeated until the root has received information from all its children. Furthermore, the proposed Algorithm 1 can be implemented via a depth-first search (DFS) initiated at v_r on \bar{G}_N .

(a) Given K_{ij} and d_i , the variation of the value of (3) against T .(b) Given K_{ij} and T , the variation of the value of (3) against d_i .Fig. 2: The variation of the value P of (3) with respect to T and d_i .

Algorithm 1 Message-Passing Algorithm for Likelihood of v_r on Tree $MP(v_r, \bar{G}_N, T)$

- 1: Let v_r be the root and send a $M_{v_r \rightarrow \text{child}(v)}^{\text{down}} = v_r.k + 1$ to its child.
 - 2: Whenever a node u receive a message from its parent, u send the message $M_{u \rightarrow \text{child}(u)}^{\text{down}} = u.k + 1$ to its child.
 - 3: Repeat 2. until every non-root node in \bar{G}_N receive a message from their parent.
 - 4: For each leaf $u \in \bar{G}_N$, set $M_{u \rightarrow \text{parent}(u)}^{\text{up}} = \int_0^T \hat{f}_u(v_r, t) dt$ and send the message $M_{u \rightarrow \text{parent}(u)}^{\text{up}}$ to $\text{parent}(u)$.
 - 5: For each pseudo-leaf $u \in \bar{G}_N$, set $M_{u \rightarrow \text{parent}(u)}^{\text{up}} = \int_0^T \hat{f}_{\text{parent}(u)}(v_r, t, d_{\text{parent}(u)} = 2) dt$ and send the message $M_{u \rightarrow \text{parent}(u)}^{\text{up}}$ to $\text{parent}(u)$.
 - 6: For each non-(pseudo)leaf and non-root node $u \in \bar{G}_N$, if u receive messages from all its children, then u send the message $M_{u \rightarrow \text{parent}(u)}^{\text{up}} = \prod_{w \in \text{child}(u)} M_{w \rightarrow u}^{\text{up}}$ to its parent.
 - 7: Return the value: $\prod_{w \in \text{child}(v_r)} M_{w \rightarrow v_r}^{\text{up}}$.
-

D. A Special Case and Properties

This section is dedicated to evaluating the analytical performance of our ML estimator derived in (5). We commence by applying (5) to a particular case: a 2-regular tree, essentially a line graph, demonstrating that our findings align with both intuitive expectations and existing literature [8], [17], as corroborated by Theorem 1. Subsequently, we delve into the ML estimator's behavior in a line-shaped rumor graph, illustrating that the likelihood value of a leaf node may either exceed or fall short of that of a centrally located node, depending on the underlying tree graph.

Proposition 1: If G is a 2-regular tree, and G_N does not contain any leaf of G . Then, the estimated rumor source of G_N is the node(s) in the middle of the line. However, if G_N contains one leaf, say v_e of G , then v_e is the estimated rumor source as time T goes to infinity.

The above proposition can either be deduced from Theorem 1 or directly computed by (5). Note that if one of G_N 's leaves is also a leaf of G , then the estimated rumor source may not be the node in the middle. The estimated source will be

on the path from the leaf to the middle node of G_N , which depends on the time T and demonstrates the ‘‘boundary effect’’ described in [14].

Next, we explore further the property of leaf nodes and pseudo-leaves. As established in Lemma 2, the value of (3) first increases and then decreases with its distance to the root, which makes characterizing the ML estimator more complicated. Let us consider a simple example where G is a general tree, and $G_N \subset G$ is a line graph with three nodes where v_y is in the middle and v_x, v_z are connected to v_y . Let d_x, d_y , and d_z denote the degree of v_x, v_y , and v_z respectively. If we treat v_y as the root, then all neighbors of v_y , except v_x and v_z , are pseudo-leaves. By considering all pseudo-leaves and leaves of G_3 we can have the closed-form expression of $P(G_3|v_i, T)$ for $i = x, y, z$ as follows:

$$\begin{aligned} P(G_3|v_y, T) &= \frac{e^{-(d_x+d_y+d_z-4)T}}{(d_x-2)(d_z-2)} (e^{(d_x-2)T} - 1)(e^{(d_z-2)T} - 1), \end{aligned}$$

and

$$\begin{aligned} P(G_3|v_z, T) &= \frac{e^{-d_z T} - e^{-(d_y+d_z-2)T}}{(d_x-2)(d_y-2)} - \frac{e^{-d_z T} - e^{-(d_x+d_y+d_z-4)T}}{(d_x-2)(d_x+d_y-4)}. \end{aligned}$$

Here we omit the close form of $P(G_N|v_x, T)$, since v_x is symmetric to v_z and $P(G_N|v_x, T)$ will be similar to that of v_z . Observe that, the formulation reduce to (2) when $d_x = d_y = d_z$, such as the constant $k = \frac{1}{(d_x-2)(d_y-2)}$ in $P(G_3|v_y, T)$. Thus, in the case of $d_x = d_y = d_z$, v_y is the ML estimator of the source for the observed G_3 . Otherwise, we can numerically show that if there is no further assumption on the degree of each node, then each of them is possible to be the ML estimator depending on their degrees. For example, when $d_x = d_z = 3$ and $d_y = 4$, we have $P(G_N|v_z, T) > P(G_N|v_y, T)$. The above example demonstrates that the number of pseudo-leaves significantly impacts the likelihood of each node in G_N . In the following, we combine the results in Lemma 1, 3 to compute the precise likelihood of nodes in a star graph.

Theorem 2: If G is a d -regular tree graph and $G_N \subset G$ is a star graph. Let v_c denote the centered node and v_p be one of its neighbors. Then, we have

$$P(G_N|v_c, T) = \frac{e^{-(N(d-2)+2)T} \cdot (e^{(d-2)T} - 1)^{N-1}}{(d-2)^{N-1}},$$

$$P(G_N|v_p, T) = \frac{e^{-(N(d-2)+2)T} \cdot (e^{(d-2)T} - 1)^{N-1}}{(N-1)(d-2)^{N-1}}.$$

The above theorem directly leads to the result that v_c is the ML estimator for the observed star graph G_N .

IV. APPROXIMATIONS AND ASYMPTOTICS BY STARLIKE TREE GRAPHS

Starlike graphs, as described by [24], are extensions of a star graph and are such that one of its spanning trees is homeomorphic to a star graph where one central node is connected to all other nodes, and these other nodes are not connected to one another. This creates a “star” pattern, with the central node as the “hub” and the other nodes as the “spokes”. In the context of online social networks like web blogs, e.g., [25]), and X (formerly Twitter), e.g., [26]–[30]), starlike graphs have also been observed to arise whereby a minority group of users (the central nodes) each has a large number of followers (the other nodes).

X (formerly Twitter) can be modeled as a social network graph, where the users are represented as nodes, and the interactions (such as following, retweeting, and replying) between them are represented as edges. This user may be an influencer or high-profile individual whose tweets attract a large following. This is known as a “scale-free” network. For example, on Twitter, the majority of users have relatively smaller follower counts as compared to the central users, and they follow the central users, thus forming the leaves of the starlike graph (so-called Superstars) [26]–[28]. Thus, X (formerly Twitter) is an illustrative example of a network with starlike graphs where influential users have numerous followers who form the network’s periphery.

The presence of these starlike structures suggests that individual influencers can have a significant impact on the cascade of information in a large online social network [26]–[30]. If a hub is an early adopter or influencer, its actions can have a disproportionate effect on the spread of information. For instance, a popular blogger sharing a new article can trigger a swift cascade of information among their numerous followers. The following result gives a necessary and sufficient condition to topologically characterize any starlike graph that we leverage to devise an algorithm for solving (1) approximately.

Theorem 3 (Corollary in [24]): A tree is starlike if and only if it has at most one vertex of degree three or more.

A starlike tree is obtained by attaching linear graphs (also called arms [13]) to this central vertex. We present a starlike approximation algorithm to transform a general graph \tilde{G}_N into a starlike tree G^* to approximate $P(\tilde{G}_N|v, T)$ of $v \in G_N$.

In Algorithm 2, we first apply the BFS graph traversal starting from v_r on \tilde{G}_N to compute the distance $d_{\tilde{G}_N}(v_r, u)$ from v_r to u for all $u \in \tilde{G}_N$. In the **for**-loop starting from line 4, we construct a new tree graph G^* based on the

Algorithm 2 Starlike Tree Approximation for $P(G_N|v_r, T)$ on General Graphs

Require: \tilde{G}_N, v_r, T

- 1: BFS(\tilde{G}_N, v_r)
 - 2: Let $G^* = \{v_r^*\}$
 - 3: $v_r^*.infected = \mathbf{TRUE}$
 - 4: **for** (pseudo)leaf $u \in \tilde{G}_N$ **do**
 - 5: Let $p_{v_r^*, u^*}$ be a path from v_r^* to u^* with length $d_{\tilde{G}_N}(v_r, u)$
 - 6: **if** u is a leaf in BFS(\tilde{G}_N) **then**
 - 7: Set all nodes on $p_{v_r^*, u^*}$ to be infected
 - 8: $G^* = G^* \cup p_{v_r^*, u^*}$
 - 9: Set $d_G^*(u^*) = d_{\tilde{G}_N}(u)$
 - 10: **else**
 - 11: Set all nodes on $p_{v_r^*, u^*}$ to be infected except u^*
 - 12: **end if**
 - 13: **end for**
 - 14: $\tilde{P}(G_N|v, T) = \text{MP}(v_r^*, G^*, T)$
-

distance $d_{\tilde{G}_N}(v_r, u)$ and the status (infected or not) for each (pseudo)leaf. We denote v_r^* and $u^* \in G^*$ as the corresponding nodes of v_r and $u \in \tilde{G}_N$. Since the **for**-loop only considers (pseudo) leaf u of BFS(\tilde{G}_N), each corresponding $u^* \in G^*$ only been considered once in line 5. Hence, the degree of $u^* \in G^*$ is at most 1 and all other nodes on the path $p_{v_r^*, u^*}$, except v_r^* and u^* , have degree at most 2. Lastly, we can observe that v_r^* is the only node in G^* with a degree possibly greater or equal to 3 since we only attach new nodes to v_r^* . By Theorem 3, we can conclude that G^* is a starlike tree. Lastly, we directly apply Algorithm 1 to G^* since it is a tree. We denote $\tilde{P}(G_N|v, T)$ as the starlike tree approximation of the likelihood $P(G_N|v, T)$.

A. Asymptotics in Performance of Likelihood Estimation

We evaluate the asymptotic likelihood ratio between two nodes in a starlike tree G_N by exploiting the asymptotic behavior of the ratio of gamma functions. We compare the true likelihood ratio $\frac{P(G_N|v_c, T)}{P(G_N|v_a, T)}$ to the likelihood ratio $\frac{\tilde{P}(G_N|v_c, T)}{\tilde{P}(G_N|v_a, T)}$ obtained by the starlike tree approximation. To simplify the analysis, we consider the starlike tree with d arms, and each arm contains k nodes, i.e., $N = kd + 1$. Let v_c denote the center of the starlike tree, and v_a be a neighbor of v_c . The likelihood ratio can be approximated by

$$\frac{\tilde{P}(G_N|v_c, T)}{\tilde{P}(G_N|v_a, T)} = \frac{(e^{-T} T^k)^d}{(e^{-T} T^{k+1})^{d-1} \cdot \frac{e^{-T} T^{k-1}}{(k-1)!}}$$

$$= \left(\frac{k+1}{T}\right)^{d-2} \cdot \frac{k+1}{k}.$$

To evaluate the asymptotic behavior of the likelihood ratio, we consider the scenario as T goes to infinity. Then we have

$$\lim_{T \rightarrow \infty} \frac{\tilde{P}(G_N|v_c, T)}{\tilde{P}(G_N|v_a, T)} = 1,$$

since $\lim_{T \rightarrow \infty} \frac{k}{T} = 1$ as $\lambda = 1$ in our assumption. Now, we consider the true likelihood ratio between v_c and v_a in the following. For the center node v_c , we have $P(G_N|v_c, T) =$

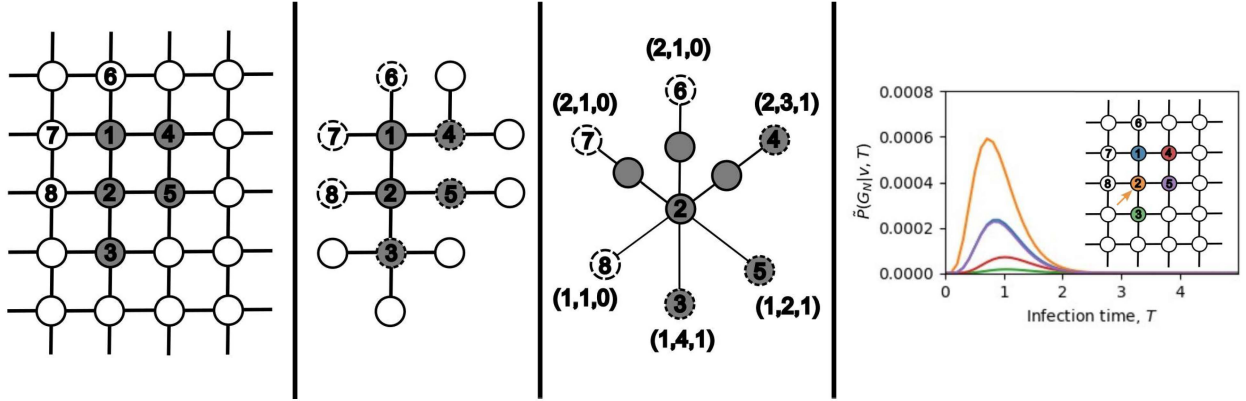


Fig. 3: An example of how Algorithm 2 works on a grid graph. We first apply the BFS graph traversal starting from the root v_2 to obtain the rumor graph and its boundary. Then, we construct the starlike tree based on the resulting BFS tree. The tuple $(k, d, 0/1)$ beside each node, say v , represents $d_{G_N}(v, \text{root}) = k$, $\text{deg}(v) = d$ and whether v is infected or not (1/0). The likelihood for each node to be the source is computed against time T . The estimated source is the node with the maximum likelihood probability over T . In this example, node 2, which is indicated by an arrow, is the estimated source. We can also observe that the curve for $\tilde{P}(G_N|1, T)$ is almost overlapping with that for $\tilde{P}(G_N|5, T)$ due to the symmetric structure of G_N .

$\tilde{P}(G_N|v_c, T)$. For v_a , we can leverage (4) to compute $P(G_N|v_a, T)$ as follows:

$$\begin{aligned} P(G_N|v_a, T) &= \frac{e^{-T} T^{k-1}}{(k-1)!} \int_0^T e^{-x} \left[\frac{e^{-(T-x)} (T-x)^k}{k!} \right]^{d-1} dt \\ &= k \cdot \left(\frac{e^{-T}}{k!} \right)^d \frac{e^{T(d-2)} T^{k-1}}{(d-2)^{k(d-1)+1}} \gamma(k(d-1)+1, (d-2)T), \end{aligned}$$

where γ is the lower incomplete gamma function. The true likelihood ratio can be computed as

$$\begin{aligned} \frac{P(G_N|v_c, T)}{P(G_N|v_a, T)} &= \frac{[T(d-2)]^{k(d-1)+1}}{k e^{T(d-2)} \gamma(k(d-1)+1, (d-2)T)} \\ &\approx \frac{T(-1)^{T(d-1)} \sum_{i=0}^{\infty} \left(\frac{d-1}{-T}\right)^{k+1} b_i(\eta) - 1}{d-2}. \end{aligned}$$

for large T, k , where $\eta = \frac{d-2}{d-1}$, and $b_0(\eta) = 1, b_1(\eta) = \eta$, $b_i(\eta) = \eta(1-\eta)b_{i-1}(\eta) + \eta(2i-1)b_{i-1}(\eta)$ [31]. The above result can be further computed by using series expansion or other asymptotic methods [32], which is beyond the scope of the present paper. We evaluate the above two likelihood ratios numerically for the case $d = 3$ in the left subgraph of Fig. 4. The right subgraph shows the tendencies of the ratio $\frac{\tilde{P}(G_N|v_c, T)}{\tilde{P}(G_N|v_a, T)} : \frac{P(G_N|v_c, T)}{P(G_N|v_a, T)}$ are similar for different value of d .

V. EXPERIMENTS

This section first provides numerical examples to illustrate the properties of the proposed estimator on starlike trees; then we compare the starlike tree approximation with existing methods in different networks.

A. Starlike tree graphs

To demonstrate the capability of simplification of the starlike tree approximation in Algo. 2, we first list out the

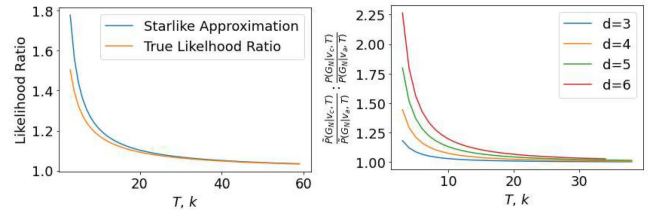


Fig. 4: The left figure is the likelihood ratios computed by the starlike approximation and the true likelihood ratio when $d = 3$ and $T = k$. Where as the right one illustrate the ratio $\frac{\tilde{P}(G_N|v_c, T)}{\tilde{P}(G_N|v_a, T)} : \frac{P(G_N|v_c, T)}{P(G_N|v_a, T)}$, for $d = 3, 4, 5, 6$.

closed form of the estimator $\tilde{P}(G_N|v, T)$ and the likelihood $P(G_N|v, T)$ for different starlike trees in Tab. I. We then plot the estimator $\tilde{P}(G_N|v, T)$ numerically in Fig. 5 and 6. From Tab. I, we can observe that when G is a line graph (a starlike tree with two arms), we have $P(G_N|v, T) = \tilde{P}(G_N|v, T)$ for all $v \in G_N$. If G has more than two arms and v is the central node of the starlike tree, then we still have $P(G_N|v, T) = \tilde{P}(G_N|v, T)$. Otherwise, the approximation $\tilde{P}(G_N|v, T)$ serves as a lower bound of $P(G_N|v, T)$ which justify the results in Lemma 3.

Fig.	v	$\tilde{P}(G_N v, T)$	$P(G_N v, T)$
5(a)	v_0	$\frac{1}{2}T^2 e^{-T}$	$\frac{1}{2}T^2 e^{-T}$
	v_1	$T(1 - e^{-T})e^{-T}$	$T(1 - e^{-T})e^{-T}$
6(a)	v_0	$T^3 e^{-3T}$	$T^3 e^{-3T}$
	v_1	$\frac{1}{4}T^4 e^{-3T}$	$(2e^T - T^2 - 2T - 2)e^{-3T}$

TABLE I: Comparison between the true likelihood $P(G_N|v, T)$ and its approximation $\tilde{P}(G_N|v, T)$, when considering starlike graphs shown in Fig. 5 and 6.

Next, we consider the case of different starlike trees G_N containing a leaf node of G . In Fig. 5 and 6, a node that

is colored in white represents uninfected nodes. Otherwise, it is infected. In the scenario where exactly one leaf node of a line graph is infected, Fig. 5 presents the maximum likelihood probability versus spreading time for each node to be the source, as approximated by the starlike tree method. The node with the highest likelihood probability over time is identified as the detected source. In each line graph in Fig. 5, node 0 is an infected leaf node of the underlying network G , and node i is connected to node $(i - 1)$ for $i \geq 1$. If there are 1 or 2 infected nodes, the detected source is node 0, the infected leaf node. However, when the number of infected nodes increases to 4 or 5, the detected source shifts to node 1, which lies on the path from the leaf node to the central node of the rumor graph. We can also observe the same phenomenon in Fig. 6c.

Fig. 6 provides an example of a starlike graph with three arms with difference lengths connected to the central node. These figures also include a curve representing $P(G_N|v, T)$ as a function of T for a selected node v . In Fig. 6a, the central node 0 is identified as the estimated source as shown in Theorem 2.

In starlike tree graphs where G_N does not contain any leaf node of G , the central node may not always be the estimated source. For example, Fig. 6c is more unbalanced than Fig. 6b regarding the size of the linear graphs attached to the central node. Consequently, the estimated source shifts from the central node 0 to the non-central node 1 in Fig. 6c. Furthermore, in starlike tree graphs, when G_N includes the leaf of G , the estimated source may shift due to the boundary effect [14]. For example, the estimated source is node 4 in Fig. 6d, which differs from that in Fig. 6c.

B. Comparison with existing methods

To assess the performance of the starlike tree approximation and compare it with existing methods, we conducted simulation experiments on the Random Trees and Erdős–Rényi (ER) random graphs. Random Tree generates a tree selected uniformly from the set of all possible trees with the given number of nodes, while the latter two models generate general graphs. In all models, we generated underlying networks with varying numbers of nodes, specifically $n \in \{50, 100, 150, 200, 250, 300\}$. For ER random graphs, we set the probability of having edges between any pair of nodes to be 0.04.

To model the rumor-spreading process, we begin by randomly selecting a node as the original source of the rumor, denoted by v^* , in each generated network. The rumor propagation over time T follows the model detailed in Section II. Our analysis aims to evaluate the starlike tree approximation's accuracy against existing methods by examining various infection ratios, specifically 0.1, 0.2, 0.3, 0.4, 0.5, and 0.6. The comparison includes methodologies such as rumor centrality with a Breadth-First Search (BFS) heuristic, distance centrality, and the Jordan center. In instances of multiple nodes computed as the source, one is chosen at random to be the detected source.

The accuracy of rumor source detection is depicted in Fig. 7. Overall, as the infection proportion increases, the accuracy of all methods tends to decrease.

In the case of random trees, the starlike tree approximation demonstrates higher accuracy compared to other methods when the infection proportion ranges between 0.2 and 0.3, and the number of nodes varies from 50 to 300. This superiority can be attributed to the starlike tree approximation's utilization of information from the boundary of the rumor graph, its consideration of the phase-type distribution of spreading, and its resistance to the boundary effect, in contrast to the rumor centrality with the BFS heuristic method. Given these characteristics, it is not surprising that the starlike tree approximation outperforms other methods in the Random Tree scenario, particularly when the number of nodes and the infection proportion is around 0.3 and 0.4.

In the Erdős–Rényi model, as depicted in Fig. 9, the starlike tree approximation demonstrates comparable accuracy across various combinations of the number of nodes and infection proportion. Notably, in the Erdős–Rényi model, the starlike tree approximation exhibits improved accuracy when the infection proportion is 0.5, and the number of nodes in the underlying network ranges from 50 to 250.

Based on our experiments, the starlike tree approximation appears to be preferred for the accurate detection of rumor sources in the Random Tree, and Erdős–Rényi model, particularly when dealing with a moderate number of nodes and infection ratio. The source code of the above simulation can be publicly accessed at <https://github.com/convexsoft/Rumor-Source-Detection>.

VI. FURTHER DISCUSSIONS

The preceding sections outline the basic contagion source detection algorithm for the exponential spreading model, allowing for diverse variations without requiring significant modifications to the algorithm or its analysis.

Examining various Markovian models for the spread of rumors in networks is crucial for comprehending information dissemination, social dynamics, and communication patterns. In addition to the exponential distribution discussed in this paper, two Markovian models suitable for analysis in this context are hyper-Erlang distributions and phase-type distributions, traditionally employed in queueing theory [33]–[35]. Hyper-Erlang distributions are a class of probability distributions that generalize the traditional Erlang distribution by allowing for more flexible shapes. In the context of rumor spreading, hyper-Erlang distributions can be used to model the inter-event times between consecutive instances of rumor transmission. This approach takes into account the varying speeds at which rumors propagate through different graph edges. By fitting hyper-Erlang distributions to empirical data on rumor propagation times, we can determine additional topological features that accelerate or slow down the spread of rumors in networks.

Phase-type distributions can be used to model complex stochastic processes of rumor dynamics by describing the transition time between different states. In the context of rumor spreading, these states could correspond to different stages of rumor dissemination, such as initial propagation, variation, and eventual fade-out. By modeling the transitions between

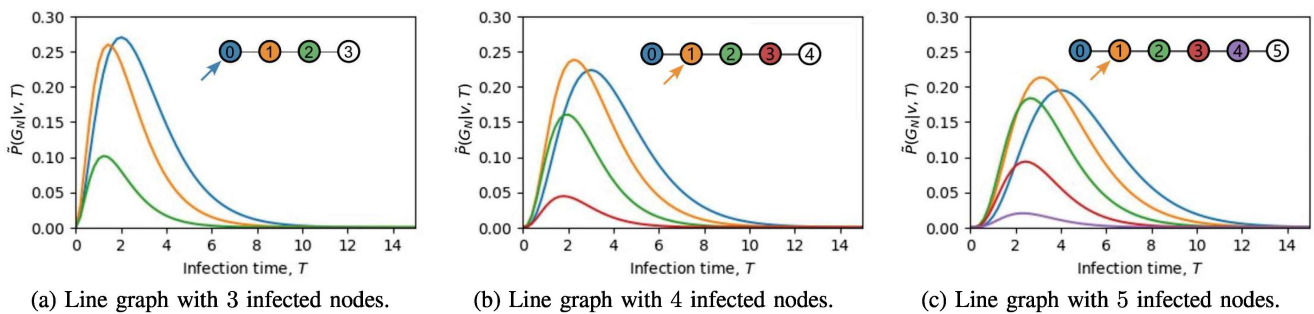


Fig. 5: $P(G_N|v, T)$ given by starlike tree approximation in line graphs where G_N contains exactly one leaf of G . The estimated sources are indicated by arrows.

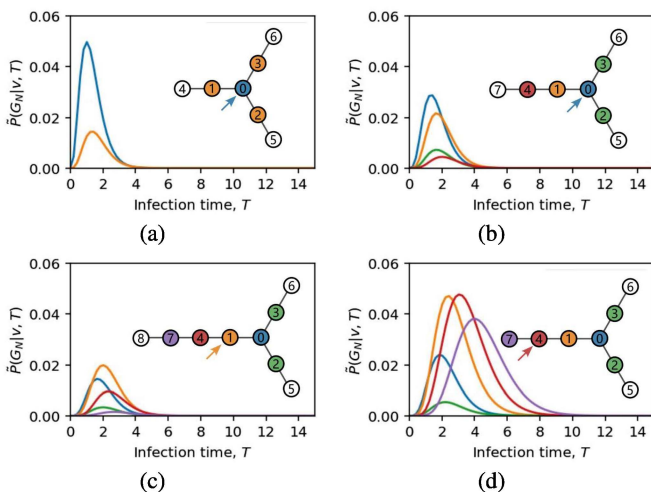


Fig. 6: $\tilde{P}(G_N|v, T)$ in star/starlike tree graphs where the central node has 3 infected neighbors. The estimated sources are indicated by arrows.

these states using phase-type distributions, we can analyze the probability of various rumor propagation scenarios based on estimated parameters such as the average time it takes for a rumor to reach a certain percentage of the network or the likelihood of a rumor dying out before spreading widely. By integrating advanced queueing-theoretic tools, more precise models of network information spreading can be developed. These Markovian spreading models can enable more robust contagion source detection by validating different models against empirical observations so as to integrate them with intervention impacts, e.g., targeted information campaigns and prediction of outbreak sizes.

Furthermore, the probabilistic inference framework in this paper can find applications in other aspects of networking. Our problem formulation possesses sufficient generality to also serve as a model for identifying the most crucial node within a network for efficient data transmission. The progression from the pivotal node to the terminal node within the infection graph can be likened to *a series of connected exponential server queues*. As a result, we can study *the selection of the source node in the network to transmit data efficiently to a specified set of terminal nodes in the shortest possible time, considering*

exponential server timing and unique service rates for each server. In particular, with a fixed aggregate service rate, the work in [36]–[39] shows that the data departure process achieves its maximum stochastic speed when all the servers in the network are homogeneous (i.e., identical Markovian model at each node). It will be interesting to combine our work with that in [36]–[39] to explore new networking applications.

Other interesting applications of the results in this paper involve correlated exponential random variables in a network, such as the Marshall-Olkin (MO) Copula Model for dependent failures and reliability assessment in networks in [40]–[42]. Hence, identifying the origin of information spreading in networks is similar to the problem of pinpointing failure points in a network [16]. For example, it is possible to use Lemma 1 and Lemma 2 in this paper with the MO Copula Model [40] to better understand the dependencies between different graph components and their susceptibility to infection or failures originating from specific sources. It will be interesting to utilize a forward engineering methodology, as described in [7], [16], along with incorporating statistical correlations within a network, to enhance the accuracy of predictions and facilitate better decision-making in designing resilient and robust networks, especially in crucial applications where cascading failures could yield substantial consequences.

VII. CONCLUSION

This work presents a comprehensive probabilistic analysis of rumor spreading in large networks, focusing on the boundary of the rumor graphs. We develop a maximum likelihood estimation approach for rumor source detection, revealing that the likelihood ratio between nodes is time-independent in degree-regular tree networks. We introduce a distributed message-passing algorithm, proven globally optimal for starlike trees and effective in general tree networks. Extending its application, we propose a starlike tree approximation method for general graphs, enhancing the algorithm's versatility in handling networks with cycles. The study utilizes gamma functions' asymptotics to analyze graph-theoretic features in extensive networks, aiding in approximating crucial combinatorial aspects for source estimation. Our extensive evaluations confirm the algorithm's robust performance in various graph structures, including those with complex cycles and bound-

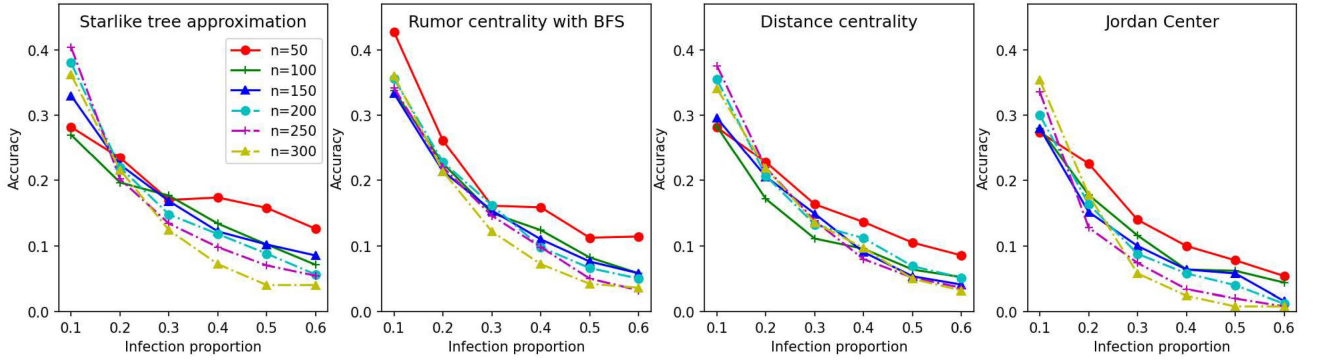


Fig. 7: Accuracy of the rumor detection methods against the infection proportion in Erdős-Rényi model.

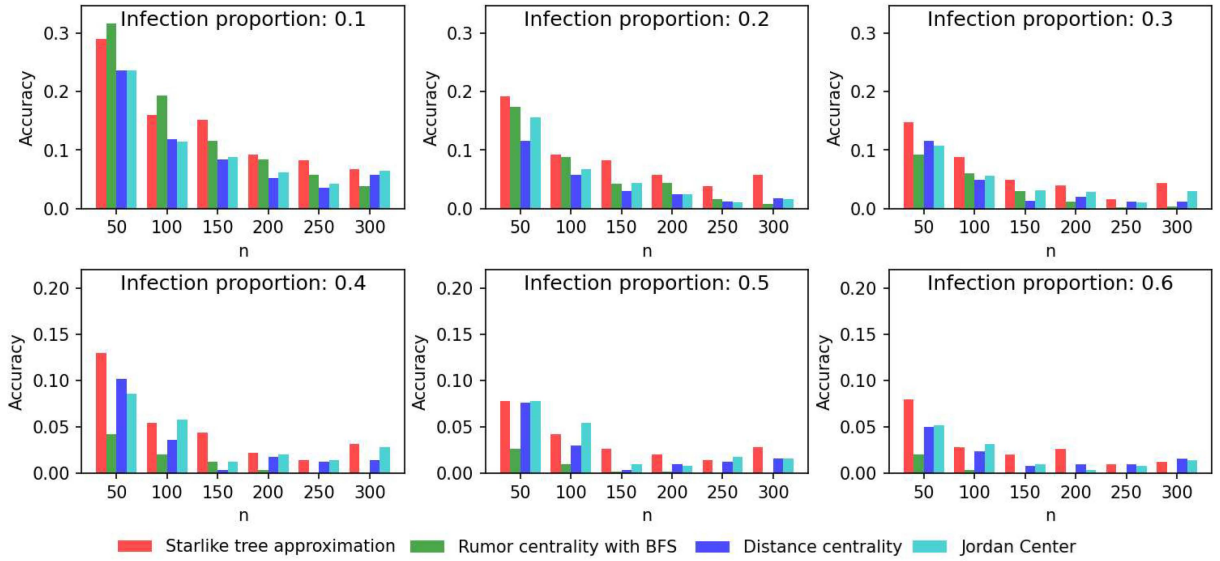


Fig. 8: Accuracy of the rumor detection methods against the infection proportion in random tree graphs.

aries, highlighting its practical applicability in diverse network scenarios.

APPENDIX

We sketch the proof of Lemma 1 as follows. We first prove that for each leaf node $v \in G_N$, the likelihood $P(G_N|T, v)$ is of the form $k \cdot e^{-(N(d-2)+2)T} \cdot (e^{(d-2)T} - 1)^{N-1}$, for some scalar k . Then, we extend the result to the non-leaf node by decomposing the original graph into several small graphs, as shown in Fig. 10.

We prove the first statement by induction on the number N . For the base case $N = 2$, we assume that G_N contains two infected nodes $\{u, v\}$, connected by an edge $e_{u,v} = a$. We denote $2(d-2)$ edges, connecting to v and u , other than $e_{u,v}$ by x_i and y_i for $i = 1, 2, \dots, d-1$ respectively. Without loss of generality, we have

$$P(G_2|T, v) = \frac{1}{d-2} e^{-(2(d-2)+2)T} (e^{(d-2)T} - 1)^{2-1},$$

where we can set $k = 1/(d-2)$. For the induction step, we assume that the statement is true when $N = s$, that is, $P(G_s|T, v) = k_s \cdot e^{-(s(d-2)+2)T} \cdot (e^{(d-2)T} - 1)^{s-1}$, where

k_s is a number only related to the network structure and v is a leaf of G_s . To construct G_{s+1} , we replace an uninfected neighbor of v with an infected node, say u . Hence, u is a leaf of G_{s+1} . By using the induction hypothesis and (4), we can compute $P(G_{s+1}|T, u)$ as follows

$$\begin{aligned} P(G_{s+1}|T, u) &= e^{-(d-1)T} \int_0^T \left[k_s \cdot e^{-(s(d-2)+1)(T-x)} \right. \\ &\quad \left. \cdot (e^{(d-2)(T-x)} - 1)^{s-1} e^{-x} \right] dx \\ &= k_s e^{-((s+1)(d-2)+2)T} \int_0^T (e^{(d-2)(T-x)} - 1)^{s-1} e^{s(d-2)x} dx \\ &= k_s e^{-((s+1)(d-2)+2)T} \int_0^T \left[\sum_{i=0}^{s-1} \binom{s-1}{i} \right. \\ &\quad \left. \cdot e^{(d-2)[T(s-1-i)+(i+1)x]} \cdot (-1)^i \right] dx. \end{aligned}$$

The first term $e^{-(d-1)T}$, after the first equation, is from the $d-1$ uninfected neighbors of u , since u is a leaf of G_{s+1} .

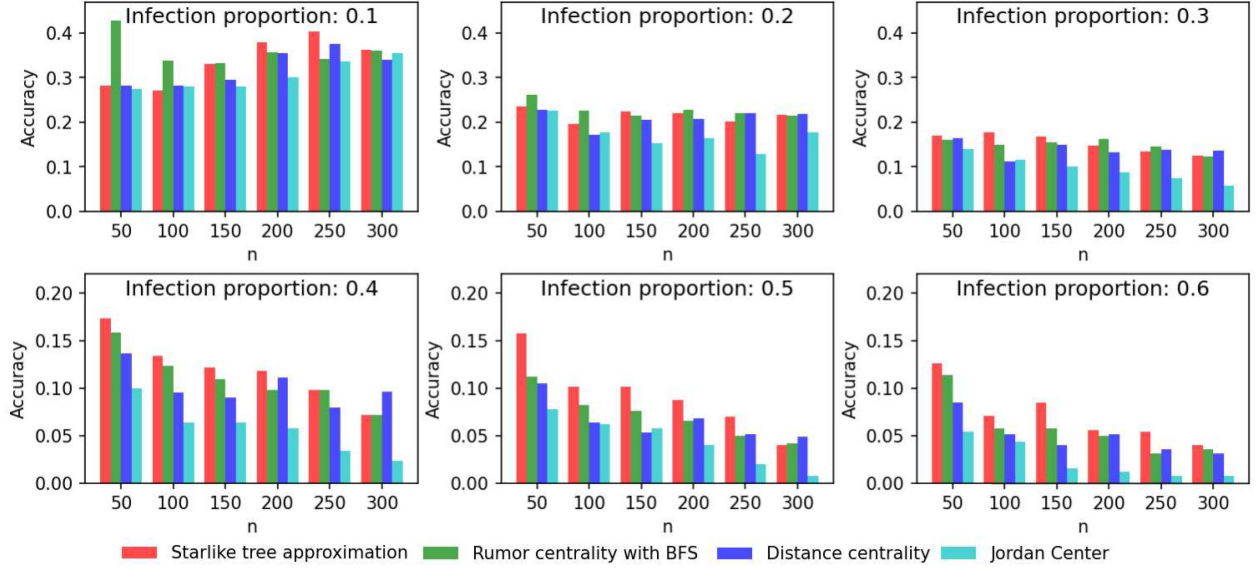


Fig. 9: Accuracy of the rumor detection methods against the infection proportion in Erdős-Rényi model.

The third equation is followed by the binomial expansion. The following is the resultant $P(G_{s+1}|T, u)$ after the integration:

$$\begin{aligned} & \frac{k_s}{d-2} e^{-((s+1)(d-2)+2)T} \left\{ \sum_{i=0}^{s-1} \left[e^{(d-2)Ts} \binom{s-1}{i} \frac{(-1)^i}{i+1} \right] \right. \\ & \quad \left. - \sum_{i=0}^{s-1} \left[\binom{s-1}{i} \frac{(-1)^i}{i+1} e^{(d-2)T(s-1-i)} \right] \right\} \\ & = \frac{k_s}{(d-2)s} e^{-((s+1)(d-2)+2)T} (e^{(d-2)T} - 1)^s. \end{aligned}$$

By setting $k_{s+1} = \frac{k_s}{(d-2)s}$, we complete the proof of the first statement. Note that from the above result, we can deduce that $\frac{P(G_{s+1}|v, T)}{P(G_{s+1}|u, T)} = \frac{s}{1}$, which is independent of T . Based on the above equation, we can compute the exact likelihood of any vertex in a degree regular tree within $O(N^2)$ complexity.

A. Proof of Lemma 1

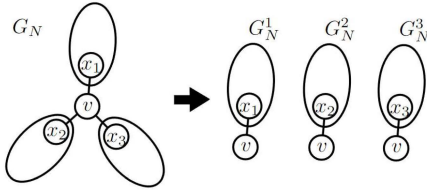


Fig. 10: Illustration of how the likelihood computation of a non-leaf vertex v with three neighboring nodes can be transformed to the multiplication of three leaf cases. Node v is not a leaf in G_N , but a leaf in G_N^1 , G_N^2 , and G_N^3 . Hence to compute $P(G_N|v, T)$, we can first decompose $P(G_N|v, T)$ as $P(G_N^1|v, T) \cdot P(G_N^2|v, T) \cdot P(G_N^3|v, T)$ then directly apply the result in leaf node to $P(G_N^i|v, T)$, for $i = 1, 2, 3$.

In the following, we extend the result to other non-leaf nodes. Given a non-leaf vertex $v \in G_N$, without loss of

generality, let $x_i \in G_N$ denote infected neighbors of v , for $i = 1, 2, \dots, d$. We consider the likelihood of v in d subtrees of G_N , say $P(G_N^i|v, T)$ separately as shown in Fig. 10, since they are independent of each other. We have

$$P(G_N^i|v, T) = \frac{k_i e^{-[(|g_{x_i}^v|+1)(d-2)+3-d]T} \cdot (e^{(d-2)T} - 1)^{|g_{x_i}^v|}}{(d-2)^{|g_{x_i}^v|}}$$

Note that in the above likelihood $P(v \cup g_{x_i}^v|v, T)$, we have removed $d-1$ uninfected neighbors from v . Hence, v has only one neighbor which is infected. We can construct $P(G_N|v, T)$ by combining the above results which leads to

$$\begin{aligned} P(G_N|v, T) &= \prod_{i=1}^d P(v \cup g_{x_i}^v|v, T) \\ &= k_v \cdot e^{-T \sum_{i=1}^d [(|g_{x_i}^v|+1)(d-2)+3-d]} \cdot (e^{(d-2)T} - 1)^{\sum_{i=1}^d |g_{x_i}^v|} \\ &= k_v \cdot e^{-(N(d-2)+2)T} (e^{(d-2)T} - 1)^{N-1}, \end{aligned}$$

where $k_v = \prod_{i=1}^d \frac{k_i}{(d-2)^{|g_{x_i}^v|}}$ and the third equation is followed by $\sum_{i=1}^d |g_{x_i}^v| = N-1$.

B. Proof of Theorem 1

Let $u, v \in G_N$ be two adjacent nodes, $x_i, y_i \in G$ are neighbors of u and v respectively for $i = 1, 2, \dots, d-1$. Since the likelihood ratio between two nodes is independent from T by Lemma 1, we can omit the term $e^{-(N(d-2)+2)T} \cdot (e^{(d-2)T} - 1)^{N-1}$. Let k_v and k_u be the scalar part of the likelihood $P(g_v^v|v, T)$ and $P(g_u^u|v, T)$ respectively. Then we have

$$\frac{P(G_N|v, T)}{P(G_N|u, T)} = \frac{k_v \frac{|g_{x_1}^v| + |g_{x_2}^v| + \dots + |g_{x_{d-1}}^v| + 1}{(d-2)^{|g_{x_1}^v| + |g_{x_2}^v| + \dots + |g_{x_{d-1}}^v| + 1}}}{k_u \frac{|g_{y_1}^u| + |g_{y_2}^u| + \dots + |g_{y_{d-1}}^u| + 1}{(d-2)^{|g_{y_1}^u| + |g_{y_2}^u| + \dots + |g_{y_{d-1}}^u| + 1}}} = \frac{|g_v^u|}{|g_u^v|},$$

where the second equation is followed by $|g_{x_i}^v| = |g_{x_i}^u|, |g_{y_i}^v| = |g_{y_i}^u|, 1 + \sum_{i=1}^{d-1} |g_{y_i}^v| = |g_v^u|$, and $1 + \sum_{i=1}^{d-1} |g_{x_i}^u| = |g_u^v|$.

C. Proof of Lemma 2

We first treat the right-hand side of (3) as a function of T , denoted as $g(T)$, with fixed $K_{i,j}$ and d_i . For brevity, we denote $K_{i,j}$ as k and d_i as d . The derivative of $g(T)$ with respect to T can be computed as follows:

$$\begin{aligned} & \frac{d}{dT} \int_0^T \frac{t^{k-1} e^{-t}}{(k-1)!} e^{-(T-t)(d-1)} dt \\ &= \frac{e^{T(1-d)}}{(k-1)!} \left(T^{k-1} e^{T(d-2)} - (d-1) \int_0^T t^{k-1} e^{t(d-2)} dt \right). \end{aligned}$$

We can omit the part $\frac{e^{T(1-d)}}{(k-1)!}$ since it is positive for all possible k, d , and T and thus will not affect the sign of the derivative. Hence, we now consider $g_1(T) = T^{k-1} e^{T(d-2)}$ and $g_2(T) = (d-1) \int_0^T t^{k-1} e^{t(d-2)}$ separately. Since v_i is a leaf of G_N but not a leaf of G , we have $d \geq 2$, and thus both $g_1(T)$ and $g_2(T)$ are strictly increasing functions. Moreover, we have $g_1'(T) \geq g_2'(T)$ for $T < k-1$, and $g_1(T) = g_2(T)$ for $T = 0$. Hence we can conclude that $g'(T) \geq 0$ initially and there is a $T^* \in [k-1, \infty)$ such that $g'(T^*) < 0$.

For the second part, we consider the case as T goes to infinity. We have

$$\begin{aligned} \lim_{T \rightarrow \infty} \frac{\int_0^T t^{k-1} e^{(d-2)t} dt}{(k-1)! e^{(d-1)T}} &= \lim_{T \rightarrow \infty} \frac{T^{k-1}}{(k-1)!(d-1)e^T} \\ &= \lim_{T \rightarrow \infty} \frac{1}{(d-1)e^T} = 0. \end{aligned}$$

Next, we prove the second property by fixing $K_{i,j}, T$, and consider the difference of (3) between the case when $d_i = D+1$ and $d_i = D$. We have:

$$\begin{aligned} & \int_0^T \frac{t^{k-1} e^{-t}}{(k-1)!} e^{-(T-t)D} dt - \int_0^T \frac{t^{k-1} e^{-t}}{(k-1)!} e^{-(T-t)(D-1)} dt \\ &= \int_0^T \frac{t^{K_{ij}-1} e^{-t}}{(K_{ij}-1)!} e^{-(T-t)D} (1 - e^{-(T-t)}) dt \leq 0, \end{aligned}$$

since $0 \leq t \leq T$ and $(1 - e^{-(T-t)}) \leq 0$.

D. Proof of Lemma 3

Suppose v_i and v_j are two leaf nodes of the rumor graph G_N given the source v_n , and we assume that v_n is the lowest common ancestor of v_i and v_j . Then, we have

$$\begin{aligned} P(v_i \cap v_j | v_n) &= \int_0^T \int_0^T \hat{f}_i(v_n, t_1) \hat{f}_j(v_n, t_2) dt_1 dt_2 \\ &= \int_0^T \hat{f}_i(v_n, t_1) dt_1 \int_0^T \hat{f}_j(v_n, t_2) dt_2, \end{aligned}$$

which implies $P(v_i \cap v_j | v_n) = P(v_i | v_n) \cdot P(v_j | v_n)$. For the second part of Lemma 3, we assume that v_n is the source and v_m is the lowest common ancestor of v_i and v_j , i.e., they are branched from v_m . We also assume that the integrand for

computing the probability of rumor spreading time from v_n to v_m , from v_m to v_i , and from v_m to v_j are $f_m(t), \hat{f}_j(v_m, t)$ and $\hat{f}_j(v_m, t)$ respectively. By the above result, the rumor spreading from v_m to v_i and from v_m to v_j are independent. Then, we have the following derivations for $P(v_i \cap v_j | v_n)$:

$$\begin{aligned} & P(v_i \cap v_j | v_n) \\ &= \int_0^T \int_0^{T-t} \int_0^{T-t} f_m(t) \hat{f}_i(v_m, t_1) \hat{f}_j(v_m, t_2) dt_1 dt_2 dt \\ &= \int_0^T f_m(t) \left(\int_0^{T-t} \hat{f}_i(v_m, t_1) dt_1 \int_0^{T-t} \hat{f}_j(v_m, t_2) dt_2 \right) dt \\ &= \int_0^T \hat{F}_i(t) \cdot \hat{F}_j(t) dF_m(t) \\ &= \int_0^{F_m(T)} \hat{F}_i(F_m^{-1}(z)) \cdot \hat{F}_j(F_m^{-1}(z)) dz \\ &\geq \frac{1}{F_m(T)} \int_0^{F_m(T)} \hat{F}_i(F_m^{-1}(z)) dz \cdot \int_0^{F_m(T)} \hat{F}_j(F_m^{-1}(z)) dz \\ &\geq \int_0^{F_m(T)} \hat{F}_i(F_m^{-1}(z)) dz \cdot \int_0^{F_m(T)} \hat{F}_j(F_m^{-1}(z)) dz, \end{aligned}$$

where $z = F_m(t)$ is the cumulative distribution function corresponding to $f_m(t)$, moreover, $\hat{F}_i(t)$ and $\hat{F}_j(t)$ are the resultant functions of t from the two inner integrals. The first inequality is followed by the Chebyshev integral inequality [43] since $\hat{f}_i(v_m, T - F_m^{-1}(z))$ and $\hat{f}_j(v_m, T - F_m^{-1}(z))$ have the same monotonicity in the range of integration according to Lemma 2. The second inequality is then followed by the fact that $F_m(T) \leq 1$. By changing the variable back to t , the second part of Lemma 3 is proved.

E. Proof of Proposition 1

Initially, we assume that the nodes in the 2-regular tree G_N are sequentially indexed as v_1, v_2, \dots, v_N . Considering that in a 2-regular tree, there are only two leaf nodes, with each leaf node connecting to one susceptible child node, the likelihood for node $v_i \in G_N$ can be simplified as

$$P(\bar{G}_N | v_i, T) = \frac{T^{i-1} e^{-T}}{(i-1)!} \frac{T^{N-i} e^{-T}}{(N-i)!}.$$

Hence, to maximize $P(\bar{G}_N | v_i, T)$ we have

$$\arg \max_{v_i \in G_N} P(\bar{G}_N | v_i, T) = \arg \min_{v_i \in G_N} (i-1)!(N-i)!,$$

that is, $\hat{v} = v_{N/2}$ if N is even; and $\hat{v} = v_{N/2-1}$ or $\hat{v} = v_{N/2+1}$ if N is odd. For the second part of the Proposition 1, without loss of generality, we assume that $v_e = v_1$, i.e., v_1 is a leaf of both G and G_N , and we consider the likelihood ratio between

v_i and v_{i+1} where $1 \leq i \leq N-1$. The likelihood ratio between two nodes is then given as follows:

$$\begin{aligned} \lim_{T \rightarrow \infty} \frac{P(\tilde{G}_N | v_i, T)}{P(\tilde{G}_N | v_m, T)} &= \lim_{T \rightarrow \infty} \frac{\int_0^T \frac{t^{i-2} e^{-t}}{(i-2)!} dt \cdot \frac{T^{N-i}}{(N-i)!}}{\int_0^T \frac{t^{i-1} e^{-t}}{(i-1)!} dt \cdot \frac{T^{N-i-1}}{(N-i-1)!}} \\ &= \lim_{T \rightarrow \infty} \frac{T(i-1) \int_0^T \frac{t^{i-2} e^{-t}}{(i-2)!} dt}{N-i \int_0^T \frac{t^{i-1} e^{-t}}{(i-1)!} dt} \\ &\approx \lim_{T \rightarrow \infty} \frac{T}{N-i} > 0. \end{aligned}$$

The last approximation is given by the fact that $\int_0^\infty t^{i-2} e^{-t} dt = \Gamma(i-1)$ and $\int_0^\infty t^{i-1} e^{-t} dt = \Gamma(i)$ along with the functional equation $\Gamma(x+1) = x\Gamma(x)$ [44]. The above result shows that as T increases to infinity when G_N is fixed, v_1 is the estimated source of G_N .

REFERENCES

- [1] A. Ganesh, L. Massoulié, and D. Towsley, "The effect of network topology on the spread of epidemics," *Proc. IEEE INFOCOM*, 2005.
- [2] S. Vosoughi, D. Roy, and S. Aral, "The spread of true and false news online," in *Science*, ser. Vol. 359, Issue 6380. USA: American Association for the Advancement of Science, 2018, pp. 1146–1151. [Online]. Available: <https://science.sciencemag.org/content/359/6380/1146>
- [3] M. D. Vicario, A. Bessib, F. Zollo, and et al, "The spreading of misinformation online," *The Proceedings of the National Academy of Sciences*, vol. 113, no. 3, p. 554–559, 2016.
- [4] S. Wasserman and K. Faust, *Social Network Analysis: Methods and Applications*. Cambridge Univ. Press, 1994.
- [5] S. van der Linden, "Misinformation: Susceptibility, spread, and interventions to immunize the public," *Nature Medicine*, vol. 28, pp. 460–467, 2022.
- [6] R. Gallotti, F. Valle, N. Castaldo, P. Sacco, and M. D. Domenico, "Assessing the risks of 'infodemics' in response to COVID-19 epidemics," *Nature Human Behaviour*, vol. 4, p. 1285–1293, 2020.
- [7] C. W. Tan and P.-D. Yu, "Contagion source detection in epidemic and infodemic outbreaks: Mathematical analysis and network algorithms," *Foundations and Trends® in Networking*, vol. 13, no. 2-3, pp. 107–251, 2023.
- [8] D. Shah and T. Zaman, "Rumors in a network: who's the culprit?" *IEEE Trans. Inf. Theory*, vol. 57, no. 8, pp. 5163–5181, 2011.
- [9] —, "Rumor centrality: A universal source detector," *SIGMETRICS Perform. Eval. Rev.*, vol. 40, no. 1, p. 199–210, jun 2012.
- [10] N. T. J. Bailey, *The Mathematical Theory of Infectious Diseases and its Applications*, 2nd ed. Griffin, 1975.
- [11] D. J. C. Mackay, *Information Theory, Inference and Learning Algorithms*, 1st ed. Cambridge University Press, 2003.
- [12] M. Fuchs and P.-D. Yu, "Rumor source detection for rumor spreading on random increasing trees," *Electronic Communications in Probability*, vol. 20, no. 2, 2015.
- [13] S. Spencer and R. Srikant, "Maximum likelihood rumor source detection in a star network," in *Proceedings of IEEE International Conference on Acoustics, Speech and Signal Processing*, 2016, pp. 2199–2203.
- [14] P.-D. Yu, C. W. Tan, and H.-L. Fu, "Rumor source detection in finite graphs with boundary effects by message-passing algorithms," in *Proceedings of IEEE/ACM International Conference on Advances in Social Networks Analysis and Mining*, ser. ASONAM '17. New York, NY, USA: ACM, 2017, pp. 86–90.
- [15] —, "Rumor source detection in unicyclic graphs," in *Proceedings of IEEE Information Theory Workshop (ITW)*, 2017, pp. 439–443.
- [16] P. D. Yu, C. W. Tan, and H. Fu, "Averting cascading failures in networked infrastructures: Poset-constrained graph algorithms," *IEEE Journal of Selected Topics in Signal Processing*, vol. 12, no. 4, pp. 733–748, 2018.
- [17] —, "Epidemic source detection in contact tracing networks: Epidemic centrality in graphs and message-passing algorithms," *IEEE Journal of Selected Topics in Signal Processing*, vol. 16, no. 2, pp. 234–249, 2022.
- [18] W. Dong, W. Zhang, and C. W. Tan, "Rooting out the rumor culprit from suspects," *Proc. of IEEE ISIT*, 2013.
- [19] W. Luo, W. P. Tay, and M. Leng, "Identifying infection sources and regions in large networks," *IEEE Transactions on Signal Processing*, vol. 61, no. 11, pp. 2850–2865, 2013.
- [20] Z. Wang, W. Dong, W. Zhang, and C. W. Tan, "Rumor source detection with multiple observations: Fundamental limits and algorithms," *Proc. of ACM SIGMETRICS*, 2014.
- [21] T.-H. Fan and I.-H. Wang, "Rumor source detection: A probabilistic perspective," in *2018 IEEE International Conference on Acoustics, Speech and Signal Processing (ICASSP)*, 2018, pp. 4159–4163.
- [22] G. Nie and C. Quinn, "Localizing the information source in a network," in *TrueFact 2019: KDD 2019 Workshop on Truth Discovery and Fact Checking: Theory and Practice*. KDD, July 2019.
- [23] L. Zheng and C. W. Tan, "A probabilistic characterization of the rumor graph boundary in rumor source detection," *Proc. of IEEE DSP*, pp. 765–769, 2015.
- [24] G. Chartrand and S. F. Kapoor, "Starlike graphs," *The American Mathematical Monthly*, vol. 74, no. 1, pp. 4–8, 1967.
- [25] J. Leskovec, M. McGlohon, C. Faloutsos, N. Glance, and M. Hurst, "Patterns of cascading behavior in large blog graphs," in *Proceedings of the 2007 SIAM International Conference on Data Mining (SDM)*. SIAM, 2007.
- [26] S. Bhamidi, J. M. Steele, and T. Zaman, "Twitter event networks and the superstar model," *The Annals of Applied Probability*, vol. 25, no. 5, pp. 2462–2502, 2015.
- [27] T. Becker, A. Greaves-Tunnell, A. Kontorovich, S. J. Miller, and K. Shen, "Viruslike dynamics on starlike graphs," *Journal of Nonlinear Systems and Applications*, vol. 4, no. 1, pp. 53–63, 2013.
- [28] A. Takigawa and S. J. Miller, "Analyzing virus dynamics on k -level starlike graphs," in *Spring 2021 AMS Eastern Sectional Meeting: Special Session on Applications and Asymptotic Properties of Discrete Dynamical Systems*, Spring 2021.
- [29] R. Rotabi, K. Kamath, J. Kleinberg, and A. Sharma, "Cascades: A view from audience," in *Proceedings of the 26th International Conference on World Wide Web (WWW)*. ACM, 2017, pp. 587–596.
- [30] B. Hooi, K. Shin, H. A. Song, A. Beutel, N. Shah, and C. Faloutsos, "Graph-based fraud detection in the face of camouflage," *ACM Transactions on Knowledge Discovery from Data (TKDD)*, vol. 11, no. 4, 2017. [Online]. Available: <https://dl.acm.org/doi/pdf/10.1145/3056563>
- [31] N. M. Temme, *Computational Aspects of Incomplete Gamma Functions with Large Complex Parameters*. Boston, MA: Birkhäuser Boston, 1994, pp. 551–562.
- [32] A. Erdélyi and F. G. Tricomi, "The asymptotic expansion of a ratio of gamma functions," *Pacific Journal of Mathematics*, vol. 1, no. 1, pp. 133–142, 1951.
- [33] H. Kobayashi, *Modeling and Analysis: An Introduction to System Performance Evaluation Methodology*. Addison-Wesley, 1978.
- [34] H. Kobayashi, B. L. Mark, and W. Turin, *Probability, Random Processes and Statistical Analysis*. Cambridge University Press, 2012.
- [35] L. Zino and M. Cao, "Analysis, prediction, and control of epidemics: A survey from scalar to dynamic network models," *IEEE Circuits and Systems Magazine*, vol. 21, no. 4, pp. 4–23, Fourth quarter 2021.
- [36] R. R. Weber, "The interchangeability of $\cdot/m/1$ queues in series," *Journal of Applied Probability*, vol. 16, no. 3, pp. 690–695, September 1979.
- [37] T. Lehtonen, "On the ordering of tandem queues with exponential servers," *Journal of Applied Probability*, vol. 23, no. 1, pp. 115–129, March 1986.
- [38] M. Kijima and N. Makimoto, "On interchangeability for exponential single-server queues in tandem," *Journal of Applied Probability*, vol. 27, no. 2, pp. 459–464, 1990.
- [39] R. R. Weber, "The interchangeability of tandem queues with heterogeneous customers and dependent service times," *Advances in Applied Probability*, vol. 24, no. 3, pp. 727–737, September 1992.
- [40] A. W. Marshall and I. Olkin, "A multivariate exponential distribution," *Journal of the American Statistical Association*, vol. 62, no. 317, pp. 30–49, 1967.
- [41] O. Matus, J. Barrera, E. Moreno, and G. Rubino, "On the marshall-olkin copula model for network reliability under dependent failures," *IEEE Transactions on Reliability*, vol. 68, no. 2, pp. 451–461, 2019.
- [42] Z. Botev, P. L'Ecuyer, R. Simard, and B. Tuffin, "Static network reliability estimation under the marshall-olkin copula," *ACM Transactions on Modeling and Computer Simulation*, vol. 26, no. 2, p. No.14, 2016.
- [43] A. M. Fink and M. J. Jr., "On Chebyshev's other inequality," *Lecture Notes-Monograph Series*, vol. 5, no. 2-3, pp. 115–120, 1984.
- [44] E. Artin, *The Gamma Function*. Dover Publications, 2015.